Anal. Chem. **2004,** *76,* 5293−5301

A Microfluidic System for Large DNA Molecule Arrays

Eileen T. Dimalanta,[†] Alex Lim,[†] Rod Runnheim,[†] Casey Lamers,[†] Chris Churas,[†] Daniel K. Forrest,[†] Juan J. de Pablo,[‡] Michael D. Graham,[‡] Susan N. Coppersmith,[§] Steve Goldstein,[†] and David C. Schwartz*[,†]

Laboratory for Molecular and Computational Genomics, Department of Chemistry, and Laboratory of Genetics, University of Wisconsin−Madison, 425 Henry Mall, Madison, Wisconsin 53706, Department of Chemical Engineering University of Wisconsin−Madison, 1415 Engineering Drive, Madison, Wisconsin 53706, and Department of Physics, University of Wisconsin−Madison, 1150 University Avenue, Madison, Wisconsin 53705

Single molecule approaches offer the promise of large, exquisitely miniature ensembles for the generation of equally large data sets. Although microfluidic devices have previously been designed to manipulate single DNA molecules, many of the functionalities they embody are not applicable to very large DNA molecules, normally extracted from cells. Importantly, such microfluidic devices must work within an integrated system to enable high-throughput biological or biochemical analysis—a key measure of any device aimed at the chemical/biological interface and required if large data sets are to be created for subsequent analysis. The challenge here was to design an integrated microfluidic device to control the deposition or elongation of large DNA molecules (up to millimeters in length), which would serve as a general platform for biological/biochemical analysis to function within an integrated system that included massively parallel data collection and analysis. The approach we took was to use replica molding to construct silastic devices to consistently deposit oriented, elongated DNA molecules onto charged surfaces, creating massive single molecule arrays, which we analyzed for both physical and biochemical insights within an integrated environment that created large data sets. The overall efficacy of this approach was demonstrated by the restriction enzyme mapping and identification of single human genomic DNA molecules.

Optical Mapping (OM) has emerged as a working single molecule system for the construction of high-resolution restriction maps from a broad range of clone types and, more recently, genomic DNA. Whole genome maps have been rapidly constructed from genomic DNA molecules directly extracted from both bacteria and unicellular parasites.[1−5] The system creates ordered restriction maps using randomly selected individual genomic DNA molecules mounted on positively charged, silanated surfaces[1−6] without the use of electrophoresis, PCR, clones, or hybridization. The surface-mounted DNA molecules are digested with a restriction endonuclease, and resulting fragments are stained with a fluorochrome and imaged by fluorescence microscopy; cleavage sites are visible as gaps between fragments, due to local coil relaxation. The integrated fluorescence intensity of the fragments is measured using digital image analysis, and an ordered restriction map of the molecule is created. Individual molecule maps are aligned and oriented to form contigs. Ordered restriction maps of an entire genome form a useful scaffold for guiding sequence assembly and for validating finished sequence. Since such maps are directly linked with the genome, they do not suffer from clone- or PCR-based artifacts, making them ideal for the assembly and validation of shotgun sequencing efforts. Previous whole-genome Optical Maps have, indeed, served in this capacity to aid large-scale sequencing efforts.[7−11] Further advance-

* To whom correspondence should be addressed. Fax: (608) 265-6743. E-mail: dcschwartz@facstaff.wisc.edu.

[†] Laboratory for Molecular and Computational Genomics, Department of Chemistry, and Laboratory of Genetics.

[‡] Department of Chemical Engineering.

[§] Department of Physics.

(1) Zhou, S.; Kvikstad, E.; Kile, A.; Severin, J.; Forrest, D.; Runnheim, R.; Churas, C.; Hickman, J. W.; Mackenzie, C.; Choudhary, M.; Donohue, T.; Kaplan, S.; Schwartz, D. C. *Genome Res.* **2003**, *13*, 2142−2151.

(2) Zhou, S.; Deng, W.; Anantharaman, T. S.; Lim, A.; Dimalanta, E. T.; Wang, J.; Wu, T.; Chunhong, T.; Creighton, R.; Kile, A.; Kvikstad, E.; Bechner, M.; Yen, G.; Garic-Stankovic, A.; Severin, J.; Forrest, D.; Runnheim, R.; Churas, C.; Lamers, C.; Perna, N. T.; Burland, V.; Blattner, F. R.; Mishra, B.; Schwartz, D. C. *Appl. Environ. Microbiol.* **2002**, *68*, 6321−6331.

(3) Lim, A.; Dimalanta, E. T.; Potamousis, K. D.; Yen, G.; Apodaca, J.; Tao, C.; Lin, J.; Qi, R.; Skiadas, J.; Ramanathan, A.; Perna, N. T.; Plunkett, G., III; Burland, V.; Mau, B.; Hackett, J.; Blattner, F. R.; Anantharaman, T. S.; Mishra, B.; Schwartz, D. C. *Genome Res.* **2001**, *11*, 1584−1593.

(4) Lai, Z.; Jing, J.; Aston, C.; Clarke, V.; Apodaca, J.; Dimalanta, E. T.; Carucci, D. J.; Gardner, M. J.; Mishra, B.; Anantharaman, T. S.; Paxia, S.; Hoffman, S. L.; Venter, J. C.; Huff, E. J.; Schwartz, D. C. *Nat. Genet.* **1999**, *23*, 309−313.

(5) Lin, J.; Qi, R.; Aston, C.; Jing, J.; Anantharaman, T. S.; Mishra, B.; White, O.; Daly, M. J.; Minton, K. W.; Venter, J. C.; Schwartz, D. C. *Science* **1999**, *285*, 1558−1562.

(6) Aston, C.; Hiort, C.; Schwartz, D. C. *Methods Enzymol.* **1999**, *303*, 55−73.

(7) Wei, J.; Goldberg, M. B.; Burland, V.; Venkatesan, M. M.; Deng, W.; Fournier, G.; Mayhew, G. F.; Plunkett, G., III; Rose, D. J.; Darling, A.; Mau, B.; Perna, N. T.; Payne, S. M., Runyen-Janecky, L. J.; Zhou, S.; Schwartz, D. C.; Blattner, F. R. *Infect. Immun.* **2003**, *71*, 2775−2786.

(8) Welch, R. A.; Burland, V.; Plunkett, G., III; Redford, P.; Roesch, P.; Rasko, D.; Buckles, E. L.; Liou, S. R.; Boutin, A.; Hackett, J.; Stroud, D.; Mayhew, G. F.; Rose, D. J.; Zhou, S.; Schwartz, D. C.; Perna, N. T.; Mobley, H. L.; Donnenberg, M. S.; Blattner, F. R. *Proc. Natl. Acad. Sci. U.S.A.* **2002**, *99*, 17020−17024.

(9) Deng, W.; Burland, V.; Plunkett, G., III; Boutin, A.; Mayhew, G. F.; Liss, P.; Perna, N. T.; Rose, D. J.; Mau, B.; Zhou, S.; Schwartz, D. C.; Fetherston, J. D.; Lindler, L. E.; Brubaker, R. R.; Plano, G. V.; Straley, S. C.; McDonough, K. A.; Nilles, M. L.; Matson, J. S.; Blattner, F. R.; Perry, R. D. *J. Bacteriol.* **2002**, *184*, 4601−4611.

10.1021/ac0496401 CCC: $27.50
Published on Web 08/12/2004

ments will improve the already high throughput approach of whole genome physical map construction, and as reported here, this was accomplished by the development of microfluidic devices designed to manipulate ensembles of very large genomic DNA molecules.

Over the past few years, we have witnessed an explosion in the area of microfluidics in terms of bringing this new technology to bear on a myriad of applications,[12−17] in addition to simulation studies that shed insight into how confined chains behave within typical microfluidic devices.[18] Traditionally, microchannels have been made by creating features on the surface of a substrate using standard photolithography techniques, followed by sealing of the substrate to another surface. Silicon can be sealed to silicon by wafer bonding[19] or to quartz by anodic bonding.[20] These methods for constructing microchannels, however, are problematic for several reasons: they require specialized instrumentation and are time-consuming; technically demanding; relatively expensive; and, most importantly, not disposable. Of recent interest are 3D structures molded from an elastomeric polymer, forming a network of microchannels through which fluids flow along the surface of a substrate.[21−29] This polymer, poly(dimethylsiloxane) (PDMS), forms reversible seals with most substrates with which it comes in conformal contact. The seal is sufficiently secure to resist leakage of liquids filling the microchannels, yet yielding to be reversible. The use of the polymer has several advantages over traditional methods for creating microfluidic devices: it is simple, rapid, inexpensive to produce, and disposable.

Previous work from this laboratory to develop single molecule arrays by fluid fixation has shown that the elongation of DNA molecules occurs within fluid flow developed within a drying droplet on charged glass surfaces.[30] Although this approach produced usable arrays from clones or PCR amplicons,[31] it was not suitable for genomic DNA molecules, which can easily span several millimeters in length. To meet this challenge, simple capillary action was employed, as developed by adding DNA solution to a glass sandwich;[2−5] however, this modality produced randomly deposited molecules and showed a high rate of overlapping molecules. This can affect sizing estimates, since fluorescence intensity is used to determine the size of DNA fragments created by restriction endonuclease digestion. The overlapping regions will have higher fluorescence intensities than nonoverlapping regions since multiple molecules lie in these regions, resulting in inflated estimates of fragment sizes. More detrimental are the optical chimeras formed from overlapping molecules. Overall, these errors can confound the facile construction of whole genome maps or reduce yields from the analysis of single molecule arrays.

Machine vision results are greatly enhanced and synergized by objects that are presented which are nearly perfect. This requires a high degree of uniformity and low noise, and such systems for single (large) molecule arrays did not exist. The principal reason we decided to address this problem in terms of images derived from single molecule arrays hinged on the need for high-throughput analysis, in which direct operator interaction with images is completely obviated. More precisely, we sought to develop a microfluidic system to directly complement our efforts to enable machine vision approaches that deal with the issues presented by large genomic DNA molecules, as evaluated by reliable object identification and segmentation. This effort required single molecule arrays that were discretely deposited and presented molecules bearing a common directionality.[2−5] We therefore reasoned that controlled capillary flow would be key to solving this problem, and this approach would also help to enable a completely automated system for genome analysis.

In this paper, we describe a new approach for elongating large single DNA molecules onto chemically modified surfaces using microchannels made out of PDMS. The microchannels were designed to present molecules in an arrayed fashion, providing a clear, dense, usable field for single molecule analysis and, when coupled with automatic data acquisition and machine vision, affords a novel means for rapid whole genome analysis. The microchannels were used to study the elongation and deposition of different sized DNA molecules adsorbed onto positively charged surfaces to demonstrate the efficacy of this new approach. We found the deposition of molecules to be uniform throughout the microchannels and that the extent of elongation showed a molecular weight dependence that was explained by a simple model. As a further demonstration of its utility, this microfluidic device was incorporated into the Optical Mapping system to rapidly generate single molecule physical maps of human DNA over 1 mm in length.

(10) Perna, N. T.; Plunkett, G., III; Burland, V.; Mau, B.; Glasner, J. D.; Rose, D. J.; Mayhew, G. F.; Evans, P. S.; Gregor, J.; Kirpatrick, H. A.; Posfai, G.; Hackett, J.; Klink, S.; Boutin, A.; Shao, Y.; Miller, L.; Grotbeck, E. J.; Davis, N. W.; Lim, A.; Dimalanta, E. T.; Potamousis, K. D.; Apodaca, J.; Anantharaman, T. S.; Lin, J.; Yen, G.; Schwartz, D. C.; Welch, R. A.; Blattner, F. R. *Nature* **2001**, *409*, 529−533.

(11) Gardner, M. J.; Tettelin, H.; Carucci, D. J.; Cummings, L. M.; Aravind, L.; Koonin, E. V.; Shallom, S.; Mason, T.; Yu, K.; Fujii, C.; Pederson, J.; Shen, K.; Jing, J.; Aston, C.; Lai, Z.; Schwartz, D. C.; Pertea, M.; Salzberg, S.; Zhou, L.; Sutton, G. G.; Clayton, R.; White, O.; Smith, H. O.; Fraser, C. M.; Adams, M. D.; Venter, J. C.; Hoffman, S. L. *Science* **1998**, *282*, 1126−1132.

(12) Beebe, D. J.; Mensing, G. A.; Walker, G. M. *Annu. Rev. Biomed. Eng.* **2002**, *4*, 261−286.

(13) Ross, D.; Johnson, T. J.; Locascio, L. E. *Anal. Chem.* **2001**, *73*, 2509−2515.

(14) Gallardo, B. S.; Gupta, V. K.; Eagerton, F. D.; Jong, L. I.; Craig, V. S.; Shah, R. R.; Abbott, N. L. *Science* **1999**, *283*, 57−60.

(15) Burns, M. A.; Johnson, B. N.; Brahmasandra, S. N.; Handique, K.; Webster, J. R.; Krishnan, M.; Sammarco, T. S.; Man, P. M.; Jones, D. J.; Heldsinger, D.; Mastrangelo, C. H.; Burke, D. T. *Science* **1998**, *282*, 484−487.

(16) Liang, Z.; Chiem, N.; Ocvirk, G.; Tang, T.; Fluri, K.; Harrison, D. J. *Anal. Chem.* **1996**, *68*, 1040−1046.

(17) Woolley, A. T.; Mathies, R. A. *Anal. Chem.* **1995**, *67*, 3676−3680.

(18) Jendrejack, R. M.; Dimalanta, E. T.; Schwartz, D. C.; Graham, M. D.; de Pablo, J. J. *Phys. Rev. Lett.* **2003**, *91*, 038102.

(19) Lasky, J. B. *Appl. Phys. Lett.* **1986**, *48*, 78−80.

(20) Gustavsson, K. *Sens. Mater.* **1988**, *3*, 143−151.

(21) Wu, H.; Odom, T. W.; Chiu, D. T.; Whitesides, G. M. *J. Am. Chem. Soc.* **2003**, *152*, 554−559.

(22) Odom, T. W.; Thalladi, V. R.; Love, J. C.; Whitesides, G. M. *J. Am. Chem. Soc.* **2002**, *124*, 12112−12113.

(23) McDonald, J. C.; Chabinyc, M. L.; Metallo, S. J.; Anderson, J. R.; Stroock, A. D.; Whitesides, G. M. *Anal. Chem.* **2002**, *74*, 1537−1545.

(24) Whitesides, G. M.; Ostuni, E.; Takayama, S.; Jiang, X.; Ingber, D. E. *Annu. Rev. Biomed. Eng.* **2001**, *3*, 335−373.

(25) Chiu, D. T.; Jeon, N. L.; Huang, S.; Kane, R. S.; Wargo, C. J.; Choi, I. S.; Ingber, D. E.; Whitesides, G. M. *Proc. Natl. Acad. Sci. U.S.A.* **2000**, *97*, 2408−2413.

(26) Delamarche, E.; Bernard, A.; Schmid, H.; Bietsch, A.; Michel, B.; Biebuyck, H. *J. Am. Chem. Soc.* **1998**, *120*, 500−508.

(27) Duffy, D. C.; McDonald, J. C.; Schueller, O. J. A.; Whitesides, G. M. *Anal. Chem.* **1998**, *70*, 4974−4984.

(28) Delamarche, E.; Bernard, A.; Schmid, H.; Michel, B.; Biebuyck, H. *Science* **1997**, *276*, 779−781.

(29) Kim, E.; Xia, Y.; Whitesides, G. M. *Nature* **1995**, *376*, 581−584.

(30) Jing, J.; Reed, J.; Huang, J.; Hu, X.; Clarke, V.; Edington, J.; Housman, D.; Anantharaman, T. S.; Huff, E. J.; Mishra, B.; Porter, B.; Shenker, A.; Wolfson, E.; Hiort, C.; Kantor, R.; Aston, C.; Schwartz, D. C. *Proc. Natl. Acad. Sci. U.S.A.* **1998**, *95*, 8046−8051.

(31) Skiadas, J.; Aston, C.; Samad, A.; Anantharaman, T. S.; Mishra, B.; Schwartz, D. C. *Mamm. Genome* **1999**, *10*, 1005−1009.

EXPERIMENTAL SECTION

Reagents. Stock YOYO-1 (1,1′-[1,3-propanediylbis[(dimethylimino)-3,1-propanediyl]]bis[4-[(3-methyl-2(3H)- benzoxazolylidene)methyl]]-, tetraiodide) in DMSO (dimethyl sulfoxide) was purchased from Molecular Probes (Eugene, OR) and was diluted in 1× TE (pH 8.0) in 20% β-mercaptoethanol. Adenovirus DNA (Type 2) was purchased from Gibco BRL (Gaithersburg, MD) and λ-DNA from New England Biolabs (Beverly, MA). Coliphage T2 DNA was supplied by D. C. Schwartz; Bac clone RS218-BAC614 was from D. Frisch. Human genomic DNA was extracted from peripheral blood using the method of Boyum,[32] and extraction from gel inserts.[33] Human genomic DNA was also extracted from a normal male lymphoblast cell line, GM07535, from Coriell Cell Repositories (Camden, NJ). The restriction endonucleases *Pac*I and *Swa*I were from New England Biolabs (Beverly, MA).

Microchannel Fabrication. Microchannels were formed by molding PDMS (poly(dimethylsiloxane), Sylgard 184, Dow Corning, Midland, MI) onto a photolithographic master as described previously.[21−29] Briefly, a negative master was created using standard photolithography techniques. The master consisted of a silicon wafer with positive reliefs made from SU-8 photoresist (MicroChem Corp., Newton, MA). A chrome mask, used to transfer the microchannel pattern onto the photoresist, was created using e-beam lithography at the University of Wisconsin Center for Nanotechnology. Although e-beam lithography was not necessary to produce the size of the features used, it was the most convenient method available to generate the chrome mask. The pattern consisted of sets of 10 parallel channels (100 μm width, 10 mm length) with triangular entrances and exits (Figure 1A). The SU-8 photoresist features were 8 μm in height. PDMS replicas were formed by curing the PDMS on the master overnight at 60 °C. An O_2 plasma treatment of the PDMS microchannels (O_2 pressure ∼0.67 millibars; load coil power ∼300 W; 36 s; Technics Plasma GMBH 440, Florence, KY) was used to render the channels hydrophilic.[26] Typical contact angles for the PDMS after plasma treatment were ∼5°. Although the plasma treatment of PDMS is not permanent (the hydrophobic nature of PDMS will return after ∼15 min in air[26]), storage in water helped extend the lifetime of the hydrophilic surface. Plasma-treated microchannels stored in ultrapure water were used within 1 week of treatment. The contact angle of these plasma-treated microchannels had increased to ∼35°, which was sufficient to support capillary action. The ends of the microchannels were cut prior to use to generate open-ended channels and facilitate capillary action.

Optical Mapping Surface Preparation. DNA molecules were attached to glass Optical Mapping surfaces that have been treated with aminosilane (see below) to confer a critical amount of positive charge at pH 8.0; this has been previously described.[34,35] Our previous work also showed that DNA elongation is modified by the concentration of aminosilane compounds used for this derivatization. Here, Optical Mapping surfaces were prepared as previously described.[1,2] Briefly, glass cover slips (22 × 22 mm; Fisher's Finest, Fisher Scientific) were racked in custom-made Teflon racks and cleaned by heating in NanoStrip (Cyantek Corp., Fremont, CA) at 80 °C for 50 min. The cover slips were rinsed extensively with high-purity, dust-free water until the effluent attained a neutral pH. Further cleaning was done by boiling the cover slips in concentrated hydrochloric acid for 6 h, which hydrolyzes the glass surface, preparing it for subsequent derivatization. The cleaned cover slips were rinsed extensively in high-purity, dust-free water until neutral pH and then individually rinsed three times in ethanol. Any unused cover slips were stored at room temperature under ethanol in polypropylene containers.

For derivatization, 30 cleaned cover slips were placed in a Teflon block, which was placed inside of a Qorpak polypropylene container. The derivatization solution was made by mixing 250 mL of distilled water with 80 μm trimethylsilane (*N*-trimethylsilylpropyl-*N*,*N*,*N*-trimethylammonium chloride, Gelest Corp., Tullytown, PA) and 33 μm vinyl silane (vinyltrimethoxysilane, Gelest Corp., Tullytown, PA) in a polypropylene bottle. The mixture was

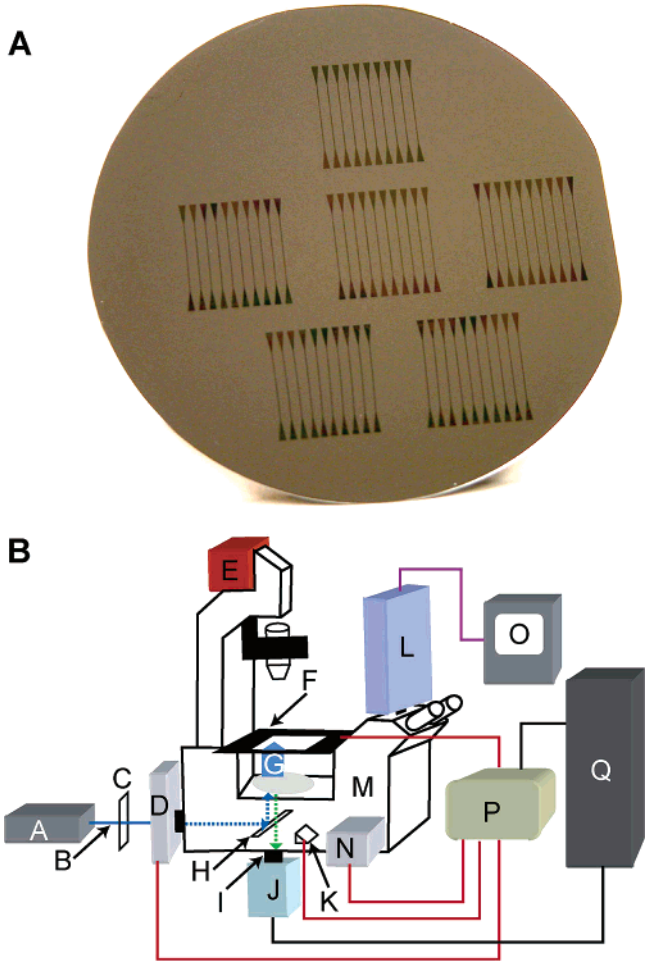

Figure 1. Experimental apparatus. 1A is an image of a silicon master with reliefs made from SU-8 photoresist. The pattern consists of six sets of 10 microchannels. 1B is a schematic of the microscope station. The parts of the station are (A) argon ion laser, (B) fiber-optic coupling, (C) λ/4 plate, (D) shutter, (E) halogen lamp, (F) $x-y$ translation stage, (G) 63× objective, (H) dichroic mirror, (I) holographic notch filter, (J) CCD camera, (K) light-path actuator, (L) SIT camera, (M) inverted microscope, (N) focus motor, (O) monitor, (P) Ludl MAC 2000 interface, and (Q) PC. The red lines indicate the parts of the microscope that are controlled by the Ludl MAC 2000 interface. The black lines show how the station is controlled by a PC. The purple line connects the SIT camera to a monitor for user visualization of the sample.

(32) Boyum, A. *Scand. J. Clin. Lab. Invest., Suppl.* **1968**, *97*, 77−89.
(33) Schwartz, D. C.; Cantor, C. R. *Cell* **1984**, *37*, 67−75.
(34) Meng, X.; Benson, K.; Chada, K.; Huff, E. J.; Schwartz, D. C. *Nat. Genet.* **1995**, *9*, 432−438.
(35) Cai, W.; Aburatani, H.; Stanton, V. P.; Housman, D. E.; Wank, Y.; Schwartz, D. C. *Proc. Natl. Acad. Sci. U.S.A.* **1995**, *92*, 5164−5168.

vigorously shaken, and then carefully poured over the 30 racked acid cleaned cover slips in the Qorpak container. The Qorpak containing the cover slips and the silane solution was incubated at 65 °C with gentle shaking (50 rpm) for 17.5 h. The container was then opened and placed in a chemical exhaust hood for 1 h to allow the temperature to equilibrate. The silane solution was aspirated, and the derivatized surfaces were rinsed 2 times with distilled water and once with ethanol. Unused surfaces were stored under ethanol.

DNA Elongation and Deposition. The PDMS microchannels were placed onto an Optical Mapping surface, which provided the "floor" of the microchannels. Microliter quantities of a DNA solution were deposited at one end of the microchannels and fully loaded by capillary action. The DNA molecules elongated in this flow and adsorbed onto the OM surface, parallel to the direction of the flow. After 10 s, the PDMS was peeled from the OM surface, and excess DNA solution was carefully aspirated from the surface. The surface-mounted DNA molecules were then stained with YOYO-1 (200 nM in 20% β-mercaptoethanol in 1× TE) and sealed onto a microscope slide with nail polish to prevent the sample from drying while imaging.

DNA Digestion. DNA molecules were deposited onto Optical Mapping surfaces using capillary action within the PDMS microchannels. Next, a thin layer of 3.3% acrylamide was applied to the surface. Upon polymerization, the surface was rinsed with 200 μL of enzymatic digestion buffer (1× NEBuffer 1 or NEBuffer 3), and the excess was carefully aspirated off the surface. A solution containing 5 μL (50 U) of *Swa*I or *Pac*I (New England Biolabs, Beverly, MA) in 200 μL of digestion buffer (NEBuffer 3 for *Swa*I; NEBuffer 1 for *Pac*I) was added on top of the acrylamide layer and incubated in a humidity chamber. For *Swa*I digestion, the surface was incubated for 2−3 h at room temperature. For *Pac*I digestion, the surface was incubated for 3−5 h at 37 °C. The enzyme solution was carefully aspirated from the surface, and the surface was washed twice with excess high-purity, dust-free water. The surface was dried in a dehumidifying chamber using desiccant (Drierite) until no solution was visible on the surface. The surface with DNA was then stained with 8 μL of 200 nM YOYO-I (200 nM in 20% β-mercaptoethanol in 1× TE) and sealed onto a microscope slide with nail polish to prevent the sample from drying while imaging.[1,2]

Instrumentation. An argon ion laser-illuminated inverted Zeiss 135M microscope was used to image the DNA molecules. The microscope was equipped with a 63× Zeiss Plan-Neofluar oil immersion objective, a Dage SIT68GL low-light-level video camera connected to a Sony monitor for visual inspection of the sample, and a Roper Scientific cooled charge-coupled device digital camera (Photometrics CoolSNAP$_{HQ}$, 1392 × 1040 pixels, Sony ICX285 chip, 12-bit digitization) for acquiring focus and high-resolution images. A Ludl Electronics $x-y$ stage and focus motor with 0.1-μm resolution was used for $x-y-z$ translation. Figure 1B is a schematic of the microscope station.

Image Acquisition. The deposition of DNA molecules in an arrayed fashion, such as that in the PDMS microchannels, has made image acquisition amenable to automation. DNA molecules were imaged using software (ChannelCollect, to be published elsewhere) developed in our laboratory to integrate microscope stage motion, focus, image collection, and file management. Control of light path actuators, focus, and sample translation was accomplished by a Ludl Electronics MAC 2000 interface bus. The researcher simply inputs the coordinates of all the microchannels on a surface, and the sample is imaged automatically. Consecutive images had a 20% overlap to ensure that usable data can be extracted from DNA molecules that are larger than one image or DNA molecules that span the intersection of images. Approximately 120 images were collected per microchannel, with 10 microchannels per OM surface. An entire surface (∼1200 images) can be acquired in <1 h due to high-intensity laser illumination and the high-speed CCD camera.

Image Processing and Machine Vision. We developed an integrated image acquisition and machine vision system to automatically detect and analyze molecules within the collected image data (to be published elsewhere). Briefly, the images were first corrected for the illumination profile of the light source used during imaging (flat field correction). Next, the images were overlapped together to form a seamless super image that guaranteed that molecules crossing image bounds were detected and positioned correctly in the next image. After the data was processed, it was analyzed using PathFinder (machine vision), a fully automated software consisting of four parts:

1. Segmentation or Thresholding. This operation to pixel intensity data discerns the boundaries of an object against a background. Histogram analysis of image pixel intensities (data is well-fit to a Gaussian) determines the variance, and then a threshold level is selected that is several times the variance multiplied by the mode of the distribution. This step roughly identifies DNA molecules against a background. Next, a filtering step works with local pixel intensity gradients to parse random pixel intensities (background noise) from the object (DNA); this step removes of the low-energy portion of the pixel intensity distribution and reduces the amount of filtering or processing in subsequent steps.

2. Identify DNA Molecule Backbone. A modified version of Dijkstra's algorithm, with appropriate boundary conditions, optimally fits a series of lines to connect object pixels (identified in part 1) to form a series of interconnected lines that closely traverse a DNA molecule backbone.

3. Identify Fragments. With molecular contours (backbones) accurately in hand, enzyme cleavage sites, manifested as submicrometer-wide gaps, are found by their distinctive morphology and fluorescence intensity profiles. A series of local measured parameters describing enhanced fluorescence intensities due to coil relaxation at molecule ends are used to parse cleavage-mediated gaps from simple fluorescence variation along a DNA backbone. This operation was obviated for molecules not digested with a restriction endonuclease.

4. Determine Mass. With "daughter" restriction fragments belonging to a "parental" molecule identified, integrated fluorescence intensity measurement on a per fragment basis determines mass according to the following: fragment (size in basepairs) = standard (size in basepairs) × [fragment integrated intensity/standard fluorescence intensity].[5] For undigested molecules, integrated fluorescence intensities were analyzed as described in the Results and Discussion.

Optical Map Alignments with Sequence. As seen in the Results and Discussion, PathFinder was also used to generate single molecule Optical Maps of surface-bound DNA digested with restriction endonucleases. Once the backbone of each molecule

was found, locations of restriction sites were determined on the basis of variations in fluorescence intensity, and the integrated intensity of each fragment was identified. Sizes were then translated from intensity units to an absolute scale (kb) by identifying nearby size standard molecules in the image whose restriction map and size are known. This produces a physical restriction map, or an Optical Map, for each molecule. These Optical Maps are then compared to in silico maps of the entire human genome by pair-wise, global alignment. The optimal alignments are determined by a dynamic programming algorithm whose objective function is motivated by a Bayesian model of the errors in the Optical Maps.[1−5,36,37] These alignments approximate solutions to the maximum a posteriori probability density. *P* values for alignments are estimated by methods analogous to those applied to nucleic acid sequence alignments.[38,39]

RESULTS AND DISCUSSION

Filling the Microchannel. Fluid flow, mediated by capillary action, is a simple and direct means for the loading of microfluidic devices. This approach obviates the need for active fluid pumping schemes, which do not readily engender simple devices for routine genome analysis. Here, we wanted to exploit such flows to uniformly deposit a large number of single DNA molecules onto an OM surface (Experimental Section) that presented a usable degree of uniformity, as characterized by an effective polymer contour length. We measured this as the apparent "length" of an adsorbed molecule. Consider that laminar flow through the microchannels can be characterized by a form of the Hagen−Poiseuille equation,

$$\bar{v} = \frac{C_g \Delta p}{\eta L} \tag{1}$$

where $\bar{v}$ is the average flow rate, C_g is a geometric form factor describing the channel, Δp is the pressure drop, η is the viscosity of the fluid, and L is the length of the channel. The pressure drop Δp can be described by the capillary pressure, given the small dimensions of the microchannel and that the microchannel is open at both ends. The capillary pressure P_c can be calculated by

$$P_c = \gamma\left(\frac{\cos(\theta_{substrate}) + \cos(\theta_{PDMS})}{a} + \frac{2\cos(\theta_{PDMS})}{b}\right) \tag{2}$$

where γ is the surface tension of the liquid, $\theta_{substrate}$ and θ_{PDMS} are the contact angles of the channel, and a and b are the height and width of the channel. This relation shows that the capillary pressure is highly dependent on the wettability of the channel. The geometric term, C_g can be approximated by

$$C_g = \frac{1}{8}\left(\frac{ab}{a+b}\right)^2 \tag{3}$$

Equations 1−3 reveal that the flow rate in the channels is dependent on the dimensions of the channel and the surface tension and viscosity of the liquid.[26] Using the values of the viscosity of water, the surface tension of water, $\theta_{substrate} = 5°$, and $\theta_{PDMS} = 35°$, the calculated time it takes to fill a microchannel (8 μm high × 100 μm ×wide × 10 mm long) is 0.41 s, a close approximation to the actual filling time of ∼0.8 s, given the rudimentary nature of the model. The longer experimental loading time may have stemmed from the approximation of the DNA solution viscosity characteristics with that of simple water. As such, the shear forces generated within the device may have accentuated the non-Newtonian characteristics of a very high molecular weight DNA solution[40] to modify flow characteristics within the device. These results suggest that further experimental and theoretical work may be warranted to fully understand the details of very long polymer chains in such systems.

Deposition of DNA Molecules onto Derivatized Surfaces. Two OM surfaces with 10 microchannels per surface were imaged and analyzed for each of the four different DNA samples. Figure 2 is an example of DNA molecules adsorbed onto OM surfaces using PDMS microchannels. A majority of the molecules are elongated and aligned parallel to the direction of fluid flow. Minimal overlapping of molecules occurred and can usually be controlled by lowering the DNA concentration in the sample. Such alignment with minimal overlapping greatly facilitates image processing and analysis.

Images were analyzed as described in the Experimental Section to study the deposition of the DNA molecules onto the OM surface by determining the position of each molecule within the microchannel. The output from PathFinder was filtered to ensure that the dataset included only individual, largely intact DNA molecules, and not background noise or broken molecules. The ratio of the integrated fluorescence intensity to the apparent length of the molecules was calculated for each sample. The mean ±10% of this ratio was kept and used for subsequent analysis. The number of images per microchannel can vary due to user-defined start and end positions of each microchannel during the setup of the collection program. For this reason, the positions of the molecules were normalized so that the data from the same DNA sample in different microchannels can be analyzed together. Each microchannel was divided into 50 equal sections, with position 1 corresponding to the entrance of a microchannel, and position 50 corresponding to the exit of a microchannel. One microchannel section is roughly 200 μm in length. The results can be seen in Figure 3, where data from all of the microchannels containing a particular DNA sample were combined. The mean deposition for adenovirus DNA (35.9 kb) was 1411 molecules, with a standard deviation of 131; the mean for λ (48.5 kb) was 481 molecules, with a standard deviation of 41; Bac614 (82.5 kb) had a mean deposition of 370 molecules, with a standard deviation of 76; and T2 (164.0 kb) had a mean of 504 molecules with a standard deviation of 42. Overall, deposition seems uniform, and there does not appear to be a preference for molecules to deposit at one end of a microchannel versus the other end. Nonuniformities in deposition (such as that in Figure 3C) can probably be attributed to nonuniformities in the microchannel surfaces (OM and PDMS).

(36) Anantharaman, T.; Mishra, B.; Schwartz, D. C. *J. Comput. Biol.* **1997**, *4*, 91−118.
(37) Anantharaman, T.; Mishra, B.; Schwartz, D. C. *Proc. Int. Conf. Intell. Syst. Mol. Biol.* **1999**, 18−27.
(38) Waterman, M.; Vingron, M. *Stat. Sci.* **1994**, *9*, 367−381.
(39) Karlin, S.; Altschul, S. F. *Proc. Natl. Acad. Sci. U.S.A.* **1993**, *15*, 5873−5877.
(40) Zimm, B. H.; Crothers, D. M. *Proc. Natl. Acad. Sci. U.S.A.* **1962**, *48*, 905−911.

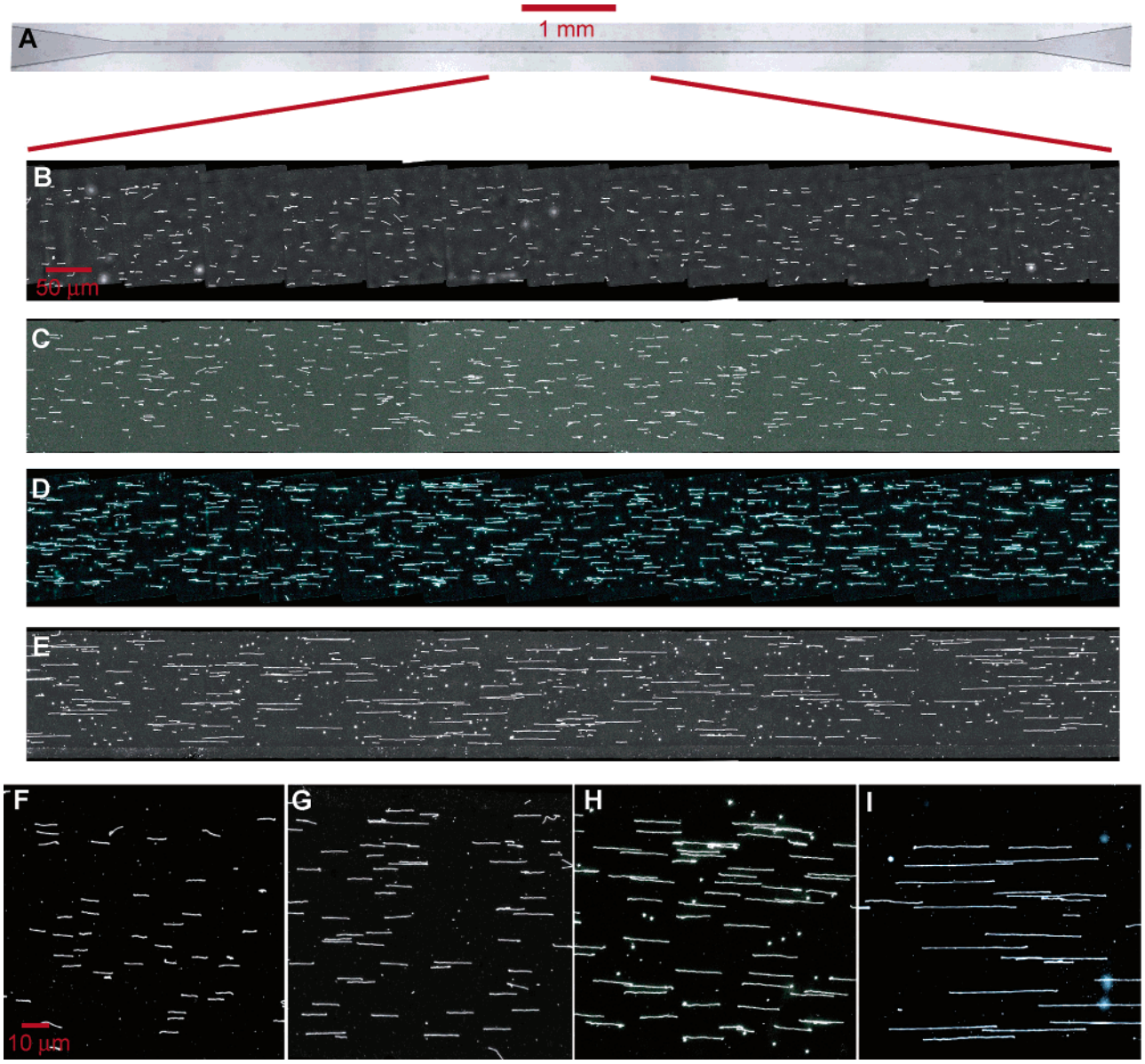

Figure 2. Views of a single microchannel and DNA deposition results. Part A is an image of a single PDMS microchannel. Parts B−E are montaged images of different DNA molecules adsorbed onto OM surfaces using capillary action within PDMS microchannels. Part B is adenovirus DNA, C is λ-bacteriophage, D is RS218 BAC614, and E is coliphage T2 DNA. Parts F−I are magnifications of small segments of the images in B−E, showing detailed views of DNA elongation.

The deposition of DNA molecules in a fluid onto an OM surface, termed fluid fixation, has been previously studied.[30] In fluid fixation, molecules elongate by the combination of fluid flows caused by the evaporation of a droplet of DNA solution, and adsorption to an OM surface. The elongated molecules adsorb onto the surface at the liquid−surface interface, in contrast with fluid meniscus-based techniques (molecular combing), where one end of a molecule attaches to a surface and elongates in the fluid−air interface that sweeps past as drying occurs.[41] Here, the driving force is the fluid flow caused by capillary forces of the microchannel, and similarly, deposition occurs at the liquid−surface interface.

In terms of deposition, the diffusion of molecules must be considered in a micrometer-sized system. The diffusion constant, D, can be described by[42]

$$D = \frac{kT}{f} \tag{4}$$

where k is the Boltzmann's constant, T is the temperature, and f is the frictional coefficient (Stokes equation of friction: $f = 6\pi\eta r_h$, where η is the viscosity of the solution and r_h is the radius of hydration). This leads to diffusion constants of $3.2-6.8 \times 10^{-9}$ cm^2/s for the DNA samples used. Here, we conservatively approximate the frictional coefficient of a DNA molecule as a random coil, since we do not know the exact conformation it adapts within the flows generated in our device. Given the

(41) Bensimon, A.; Simon, A.; Chiffaudel, A.; Croquette, V.; Heslot, F.; Bensimon, D. *Science* **1994**, *265*, 2096−2098.

(42) Cantor, C. R.; Schimmel, P. R. *Biophysical Chemistry*; W. H. Freeman and Company: New York, 1980; Chapter 10.

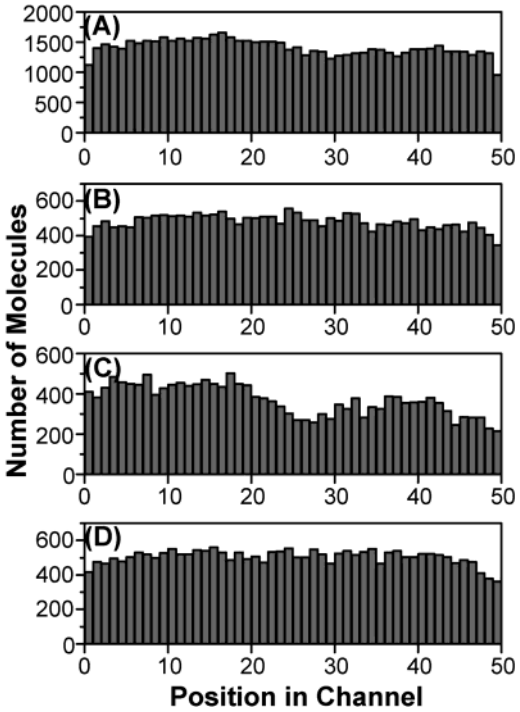

Figure 3. Histograms showing DNA deposition densities within microchannels. Position 1 is at the entrance of the microchannel, and position 50 is at the exit of the microchannel. Part A corresponds to adenovirus DNA, B to λ-bacteriophage, C to RS218 BAC614, and D to coliphage T2.

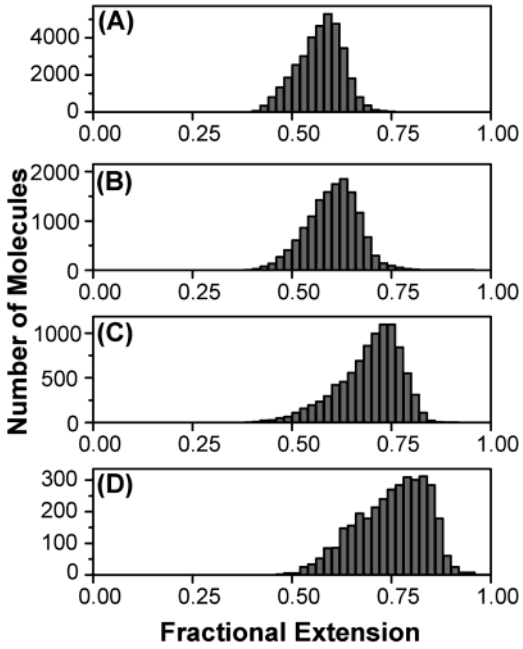

Figure 4. Fractional extension of DNA molecules. Parts A−D are histograms of the fractional extension of different DNA molecules on OM surfaces. Part A corresponds to adenovirus DNA, B to λ-bacteriophage, C to RS218 BAC614, and D to coliphage T2.

equation for the root-mean-square distance traveled by a diffusing molecule ($\langle x \rangle = \sqrt{2Dt}$), on average, the DNA molecules can diffuse ~3.1 μm toward the surface, given the residence time of the molecules in the channel. Therefore, on average, only molecules within 3.1 μm of the surface can adsorb onto the surface, and most of the molecules in the solution do not attach to the surface within the microchannel. For instance, λ-DNA can diffuse ~3.4 μm toward the surface. The concentration of λ-DNA used for the experiment was ~25 pg/μL, or roughly 0.2 pg of DNA in a completely filled microchannel. Assuming there is an equal distribution of molecules within the channel, there is ~0.085 pg of DNA that could diffuse toward the surface and attach to the surface. On average, the actual amount of DNA that attached to the surface in one microchannel was 0.05 pg. This estimate was determined by taking the total amount of DNA (apparent length in pixels as outputted by PathFinder) and multiplying this sum by the average fractional extension of λ (500 basepairs/pixel; further described in the following section); this value was converted to mass and then divided by the total number of channels. Similarly, given the concentration of adeno used (50 pg/μL) and the diffusion constant of adeno (6.8×10^{-9} cm^2/s), 0.19 pg DNA could diffuse toward the surface and attach to the surface. On average, the actual amount of adeno that adsorbed to the surface in one channel was 0.14 pg. The reason the amount of DNA on the surface is less than the calculated value is most likely due to the fact that not all molecules productively adsorb to the surface. A majority of the sample either attaches to the surface at the wider, triangular region of the channel (which does not get imaged), or is aspirated off the surface once the PDMS microchannel has been peeled from the OM surface. It was not possible to accurately relate the diffusion of Bac614 and T2 with deposition due to the fact that upon dilution of these DNA samples, their exact concentration is ill defined. This is because the experiments required DNA molecules to be as intact as possible. Therefore, thorough mixing of these two DNA samples was avoided in order to minimize any breakage of the molecules due to shear. However, it can be reasoned that the larger molecules, such as Bac614 and T2, will behave similarly to the smaller molecules, such as λ and adeno, in that most of the sample does not deposit onto the Optical Mapping surface.

Elongation. Images were analyzed as described above using the fluorescence intensity-to-length ratio to include only DNA molecules in the dataset. A second filter, a histogram mode ±20% of integrated fluorescence intensity, was necessary to ensure that the dataset included only intact DNA molecules and not broken or chimeric molecules. Simple mechanical manipulations, such as diluting and pipetting the sample, can cause breakage in long molecules, such as Bac614 and coliphage T2, which are more sensitive to shear. There was also evidence of degradation in the stock adeno and T2 samples used (gel data, not shown). These broken molecules, although present in the sample prior to elongation and deposition on an OM surface, can easily be excluded from the dataset using the integrated fluorescence intensity filter. Chimeric molecules can occur on the surface when one molecule adsorbs onto the surface, overlapping the end of another molecule. Since the elongation of intact DNA molecules was the focus here, data from broken molecules, chimeric molecules, and concatemers (such was the case for the λ-bacteriophage sample) were not included. Finally, length was converted to fractional extension by dividing the apparent length (determined by PathFinder) by its corresponding calculated polymer contour length. The results can be seen in Figure 4. The mean fractional extension for adeno, the smallest DNA sample, was 0.57; λ was 0.60; Bac614 was 0.70; and T2, the largest sample used, was 0.75. Table 1 is a summary of the results seen in Figure 4. As can be

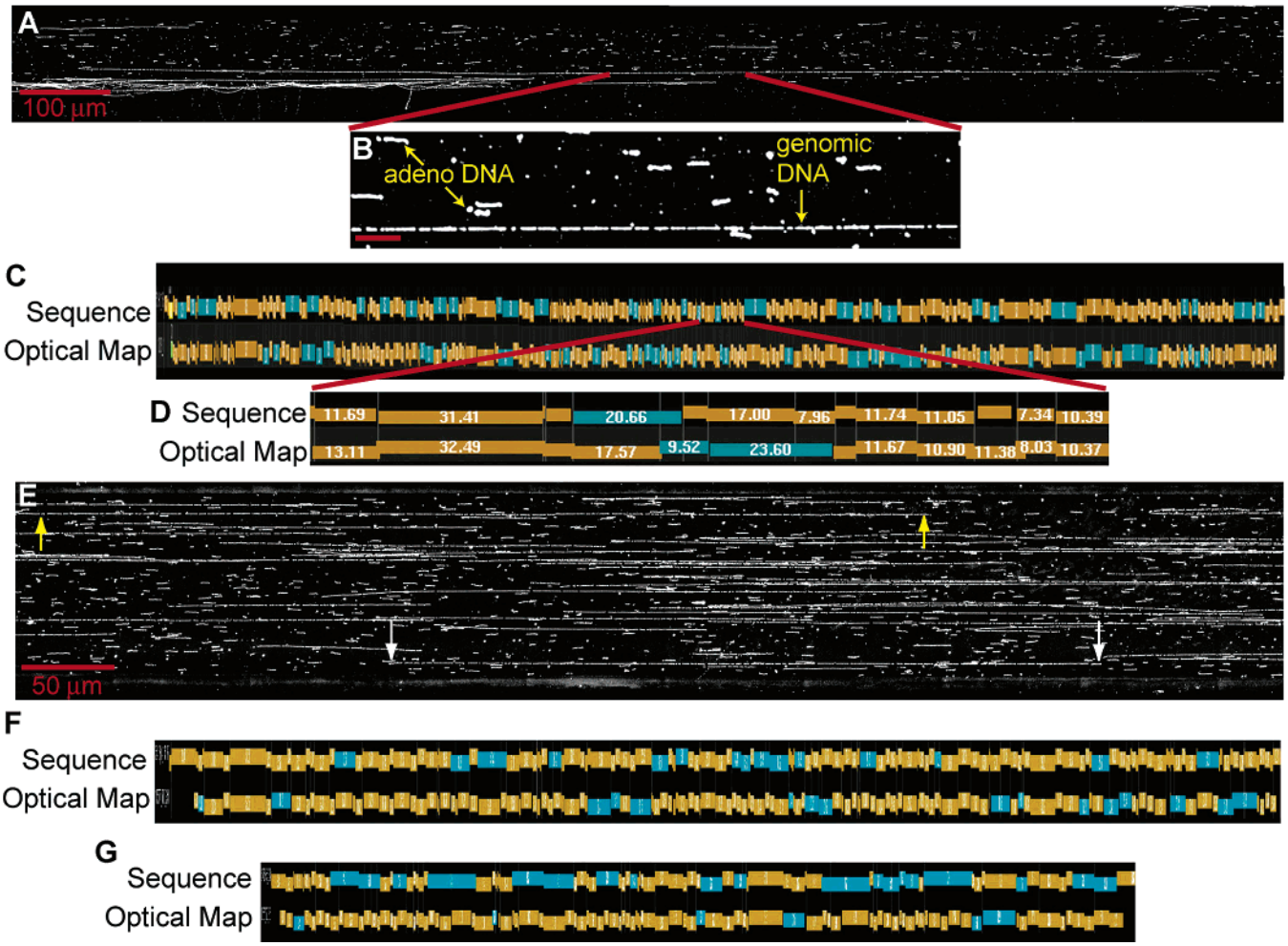

Figure 5. Human genomic DNA molecules in microchannels. Part A is fluorescence micrographs of human genomic DNA molecule deposited on an OM surface using PDMS microchannels. The surface-bound DNA molecules were cut with the restriction endonuclease *Pac*I. Part B is a magnification of a portion of the large molecule in A. Adenovirus DNA was co-mounted on the surface as a sizing standard; bar, 50 μm. Part C is a view of the alignment of the Optical Map of the molecule in A with an in silico digest of human sequence data. Part D is a magnification of C. Each bar represents a fragment produced by the restriction endonuclease, and numbers on each bar represent the size (kb) of the fragment. Part E is fluorescence micrographs of human genomic DNA digested with *Swa*I. Parts F and G show alignments between the Optical Maps and sequence.

Table 1. Fractional Extension of DNA Elongated in a Microchannel

DNA	size (kb)	no. molecules analyzed	mean fractional extension	median fractional extension	SD	histogram mode	theor fractional extension
adeno	35.9	35 309	0.570	0.576	0.056	0.59	0.62
lambda	48.5	14 200	0.603	0.607	0.065	0.63	0.67
Bac614	82.5	9211	0.695	0.710	0.079	0.73	0.76
T2	164.0	3474	0.751	0.763	0.088	0.79	0.83

seen from the results in Figure 4 and Table 1, there is a trend toward greater fractional extension with increasing molecular weight of DNA. The dependence of fractional extension on polymer length that we observe is consistent with being caused by fluid shear, if one keeps in mind that the DNA first attaches to the surface at one end, and then the rest of the polymer adheres to the surface sequentially. As more of the polymer adheres, the unbound length decreases; hence, the fractional extension of the unbound length also decreases. If one assumes that the attached segments are small and the relation between the length of a given region as it adheres and the amount of unbound polymer remaining is given by the equilibrium relation derived for polymers of fixed length, then there is a simple relation between the fractional extension in our experiments to the steady-state extension in a bulk shear flow. Consider that N is the total number of base pairs in the polymer and R is the total apparent length (as measured) of the polymer attached to the surface, then an equilibrium relation between R and N can be described as

$$\frac{R}{N} = 1 - f(N) \tag{5}$$

Given that n is the number of base pairs of unbound polymer, r is the apparent length of attached polymer, and assuming that locally the extension takes its equilibrium value where $(\delta r)/(\delta n) = 1 - f(n)$, then

$$R = \int_0^N \mathrm{d}n(1 - f(n)) = N - \int_0^N f(n)\,\mathrm{d}n \tag{6}$$

or

$$\frac{R}{N} = 1 - \frac{1}{N}\int_0^N f(n)\, \mathrm{d}n \tag{7}$$

Ladoux and Doyle[43] report for DNA tethered at one end in a shear flow experimental results that are consistent with their proposed wormlike chain scaling. They show that

$$\frac{R}{\mathrm{aN}} = 1 - C(\dot{\gamma}\tau)^{-1/3} \tag{8}$$

where aN is the contour length of the polymer, $\dot{\gamma}$ is the shear rate in seconds^{-1}, τ is the relaxation time, and C is a constant that Ladoux and Doyle find experimentally to be ~1.2 to 1.3. Using the standard scaling for the relaxation time,[44] $\tau = 1.25 \times 10^{-9}$ $\mathrm{N}^{5/3}$, with N the DNA length in base pairs, L is the contour length (aN), and using the value $C = 1.3$, one obtains

$$\frac{R}{L} = 1 - 1207(\dot{\gamma}N^{5/3})^{-1/3} \tag{9}$$

For the shear rate in our experiments of 9000 s^{-1}, this formula predicts fractional extensions of 0.62, 0.67, 0.76, and 0.83 for adeno, λ, Bac614, and T2, respectively, in good agreement with the data. This agreement is reasonable, though not definitive, because of uncertainties in the polymer relaxation time because of polymer stretch and confinement.[45] Although there appears to be a disparity in the number of molecules analyzed between the different DNA samples, the total amount of DNA analyzed for each sample was comparable.

Applications to Optical Mapping. Incorporating PDMS microchannels into the Optical Mapping system has provided a means to rapidly analyze genomes. Deposition of DNA molecules onto a surface in an arrayed fashion has made possible the automation of rapid data acquisition, thus greatly minimizing user intervention. Moreover, improvements in machine vision (identifying DNA molecules) were facilitated due to the fact that the molecules have a predominant directionality. As such, PDMS microchannels have been used to rapidly generate Optical Maps of whole genomes.[1,2] Figure 5 is an example of how microchannels were used to create Optical Maps of genomic DNA. Human genomic DNA was deposited onto OM surfaces using capillary action in the microchannels. The surface-bound DNA was then digested with restriction endonucleases *Pac*I or *Swa*I, stained with YOYO-I, and automatically imaged and analyzed as described in the Experimental Section. Part A is a montaged image of fluorescence micrographs spanning an entire DNA molecule, which is 3.9 megabases in size, or roughly 1.3 mm in length. Part B is a magnification of a portion of the molecule in A. Part C is a Genspect (a map viewer-developed in our laboratory) view of the Optical Map of the molecule in A and its alignment with sequence. The molecule in A is from the long arm of chromosome 21 and starts at nucleotide 14966722 ($P \ll 10^{-7}$). Part D is a magnification of the Genspect view in C. The top set of bars represent an in silico digest of human sequence. The bottom set of bars represent the Optical Map. Each bar represents a DNA fragment generated by *Pac*I, with the corresponding size of the fragment listed in kilobase. The brown bars represent regions where both maps contain *Pac*I sites, and the blue-green bars represent regions where one map is missing a *Pac*I site. The differences in the maps are due to the errors associated with an individual molecule Optical Map. As shown previously,[1−5] the Optical Mapping system can compensate for missing or extraneous cut sites in an individual molecule map by evaluating ensembles of molecules, where the final map is constructed so that each cut site is represented by several molecules. Redundancy at each cut site also ensures that any differences between Optical Maps and sequence are confidently called and are not an artifact of the Optical Mapping system. Part E is a montaged image of a portion of a microchannel. This image contains 12.6 mb of human genomic DNA, or roughly 0.4% genome equivalent. Part F shows the alignment of the molecule in E flanked by yellow arrows with an in silico digest of sequence. This molecule is over 1.6 mb in length and is from the long arm of chromosome 4, starting at nucleotide 84887895 ($P \ll 10^{-10}$). Part G shows the alignment of the molecule in E flanked by white arrows with an in silico digest of sequence. This molecule is almost 1.3 mb in length and is from the long arm of chromosome 5, starting at nucleotide 135330070 ($P = 10^{-3}$).

CONCLUSIONS

Systems that deposit DNA molecules are playing a major role in the biological sciences through the widespread use of microarray analysis in both expression and genomic analysis. Given the push for increasingly miniaturized systems, individual DNA molecules are becoming the principal analyte, and to meet this challenge, robust arraying approaches must be developed that are matched with equally robust detection schemes. Although imaging is a potentially high-throughput means for single molecule detection, machine vision techniques are often hampered by poor presentation of molecules, and this prevents the efficient construction of large single molecule datasets—a necessary prerequisite for any statistically meaningful measurement. Here, we have shown that our microfluidic system created single molecule arrays that synergistically worked with machine vision to effectively transform image files into tabulated data that enabled large single molecule data sets to be analyzed. These results established an empirical relationship between DNA size and elongation that agreed with scaling relationships developed within this paper. Finally, the overall utility of this microfluidic system was demonstrated by the mapping of large DNA molecules, derived from human cells. The alignment of these data with sequence points the way to new modes of whole genome analysis using ensembles of single molecules.

ACKNOWLEDGMENT

We thank Jessica Severin for the development of image and data browsers and David Fryer for his assistance with the photolithography. This work was supported by grants from NIH (7-R01 HG00225-09, R01 CA79063-03; D.C.S.), DOE (DE-FG02-99ER62830; D.C.S.), and NSF (DMR-0209630; S.N.C.).

(43) Ladoux, B.; Doyle, P. S. *Europhys. Lett.* **2000**, *52*, 511−517.
(44) Klotz, L. C.; Zimm, B. H. *J. Mol. Biol.* **1972**, *72*, 779−800.
(45) Jendrejack, R. M.; Schwartz, D. C.; Graham, M. D.; de Pablo, J. J. *J. Chem. Phys.* **2003**, *119*, 1165−1163.

Received for review March 5, 2004. Accepted July 6, 2004.
AC0496401